Journal of Structural Geology, Vol. 15, Nos 3–5, pp. 293 to 307, 1993
Printed in Great Britain

0191-8141/93 $06.00+0.00

The influence of initial fold geometry on Type 1 and Type 2 interference patterns: an experimental approach

DJORDJE GRUJIĆ

Geologisches Institut, ETH, 8092 Zürich, Switzerland

(*Received* 6 *January* 1992; *accepted in revised form* 22 *July* 1992)

Abstract—Experiments on superposed folding were performed in a plane strain–pure shear rig using paraffin wax as an analogue for rocks. A series of pre-formed cylindrical folds were refolded with the compression direction acting parallel to the initial fold hinge direction, the intermediate axis perpendicular to the first fold axial plane and the extension direction parallel to the first fold axial plane and perpendicular to its axis (Type 1 interference geometry). Roundness, tightness and amplitude were varied to investigate the influence of first-fold geometry on the interference patterns. Experimental folding of an initially planar layer oriented parallel to the first-fold envelope provides a reference geometry for comparison. The results suggest that hinge roundness has less influence on the interference pattern than other factors. Close initial folds refold into Type 2 interference patterns, which become even more pronounced as the tightness increases; open folds produce Type 1 interference patterns. Folds with the same interlimb angle and the same roundness produce different interference patterns depending on relative amplitude: folds with relatively large amplitude are refolded into Type 2 patterns, whereas folds with small amplitude give clear dome and basin structures.

In a second set of experiments, the compression direction also acted parallel to the first-fold hinge, but the orientations of the intermediate and extension axes were interchanged. The interference patterns obtained are very similar to those in Type 1 interference geometry, suggesting that the major factor in determining whether Type 1 or Type 2 interference patterns develop is the initial fold geometry and not the kinematics of the second deformation.

INTRODUCTION

WITH the growing interest in understanding the geometry and deformation history of multiply deformed terrains during the 1950s, the need for experimental work in the field of superposed folds became apparent. Reynolds & Holmes (1954) produced the very first experiments on fold interference using layered plasticine models. Although scaled, their two models were not performed under controlled laboratory conditions. They were made in order to understand the geometry of 'mirror-image fold-forms' (what later became the 'crescent-and-mushroom' interference pattern) found in the field. In a series of experiments investigating laminar folding by card decks, O'Driscoll (1962a–d, 1964a,b) produced models which were designed to understand the geometry that results from superposition of two generations of similar folds. He considered in detail the two- and three-dimensional aspects of what are now referred to as Type 1 and Type 2 interference patterns. These experiments assumed passive layer behaviour. Nevertheless, together with detailed field work, mostly in the Scottish Highlands, they provided the basis for a geometrical classification of interference patterns (Ramsay 1962a, 1967). Further progress in this direction of modelling occurred during the 1980s using computer simulations (Thiessen & Means 1980, Thiessen 1986, Charlesworth 1987, Perrin *et al.* 1988). The first buckling experiments on superposed folds were undertaken by Ghosh & Ramberg (1968). They were designed to study the effects of simultaneous shortening in two or in all directions in the plane of the competent layer as well as the superposition of buckle folds formed in two periods of deformation. In a later paper (Ghosh 1974), similar experiments on the superposition of two generations of buckle folds were produced together with a study of the deformation of an earlier lineation and of the strain distribution in superposed folds. Skjernaa (1975) showed that the conclusions based on the shear fold model are not appropriate to situations in which layer buckling is active. With analogue models, she analysed the mechanical influence of first-generation folds. A further study which demonstrated the control on superposed buckling mode exerted by early fold shapes was carried out by Watkinson (1981). Most recently, in a series of experiments, going from Type 1 to Type 0 interference geometry, Odonne (1987) and Odonne & Vialon (1987) showed how early fold shape and orientation determine the second fold axis orientation, the type of interference pattern and the mechanism of superposed folding. These experiments are also important in that they were performed with the same material (paraffin wax) and a similar viscosity contrast (600:1) as those utilized in this work, facilitating a direct comparison of results.

In overview, all these previous studies modelled fold superposition with a Type 1 interference geometry and the transition to Type 0 interference geometry (Ghosh & Ramberg 1968, Skjernaa 1975, Odonne 1987, Odonne & Vialon 1987, Ghosh *et al.* 1992). With the exception of the models of Watkinson (1981) and Ghosh *et al.* (1992), all the first-phase folds were produced by experimental deformation of single- or multi-layer models. Thus, there was not much control on initial fold shape and size. In other words, both the first- and second-phase folds would theoretically be the same, if competence contrast

and layer thickness were the only controlling factors. The initial folds produced in this manner were not perfectly cylindrical—the presence of initial perturbations influenced both the shape and distribution of initial folds (e.g. Abbassi & Mancktelow 1990). The results of experiments performed over the past 20 years are consistent, however, and can be summarized as follows.

(1) If the layers are mechanically active, the initial folds do not act as passive markers during the second deformation. On the contrary, they have a strong influence on the development of the superposed folds (e.g. Ghosh & Ramberg 1968, Skjernaa 1975, Watkinson 1981).

(2) The shape and curvature of the initial fold profile determine the buckling mode during the second deformation: open rounded folds tend to refold into Type 1 interference patterns, tight angular folds tend to refold into Type 2 interference patterns (e.g. Ghosh & Rambert 1968, Skjernaa 1975, Watkinson 1981).

(3) If the axial plane of the initial folds is deformed, the superposed folds tend to be cylindrical when superposed on tight to isoclinal initial folds, but non-cylindrical when superposed on open initial folds (Ghosh 1974, Skjernaa 1975).

(4) If the axial plane of an early fold is deformed, strong shear strains develop along the hinge zones of those early folds that are located at the limbs of the later folds. This will locally rotate any lineation which was not parallel to the first fold hinge line into parallelism with it (Ghosh 1974).

(5) The length of arc of the later superposed folds depends on the original radius of curvature of the first-phase concentric folds (Ghosh 1970).

(6) If the angle between the second compression direction and the initial fold axes is small (0–30°), superposed folding is produced (i.e. Type 1). The second-generation folds have a tendency to form perpendicular to the first-generation folds rather than perpendicular to the bulk compression direction (Skjernaa 1975, Odonne & Vialon 1987).

(7) If the angle between the second compression direction and the initial fold axes is between 30° and 60°, the superposed folds become ill defined and sporadic. In this situation the second-generation folds tend to form parallel to the existing folds rather than perpendicular to the compression. The superposed folds appear in two ways: (i) they form with their orientation close to that of the initial folds which act like a strong linear anisotropy and themselves continue to develop; (ii) some open initial folds may become second-generation folds directly when a hinge from the first stage migrates and is replaced by another which then becomes part of the set of superposed folds (Odonne & Vialon 1987).

(8) If the angle between the second-phase shortening direction and the initial fold hinges is larger than 60° superposed folds do not form at all and initial folds are simply tightened (Type 0 interference pattern) (Odonne & Vialon 1987).

Even though the results of these experiments are consistent they are not complete. So far only two strain geometries (the strain geometry refers to the orientation of the initial fold hinge and axial plane with respect to the *XYZ* bulk strain axes of the second deformation) out of four have been modelled; except in two cases (Watkinson 1981, Ghosh *et al.* 1992), the shape of the initial folds has not been varied systematically; the problem of strain compatibility in sideways buckling of two differently inclined planes, commented upon by Ramsay (1967, pp. 546–548) and also foreseen by Ghosh (1974), still has not been solved. It remained, therefore, to carry out a series of experiments under tightly controlled boundary conditions in which the shape (tightness, roundness) and size (amplitude (*A*), wavelength (*W*) and arc length (*Wa*)) of initial folds were varied, for the range of possible strain geometries.

EXPERIMENTAL PROCEDURE

The scale-model experiments were performed following the principles developed by Hubbert (1937) and Ramberg (1981), in a plane strain–pure shear deformation rig as described by Mancktelow (1988a). Experiments were conducted under two sets of conditions:

(a) low viscosity contrast experiments (17:1): at 24 ± 0.1°C, constant natural strain rate of 3×10^{-5} s^{-1} and with confining stress of 0.3 bar (0.03 MPa);

(b) high viscosity contrast experiments (≈600:1): at 29 ± 0.1°C, constant natural strain rate of 1.5×10^{-5} s^{-1} and with the same confining stress of 0.3 bar (0.03 MPa). Except when specifically noted, all the experiments were performed under these conditions.

Differential stress ($\sigma_1 - \sigma_3$), confining stress, temperature and strain rate were recorded during the experiments. All the models were shortened by 36%. Since the models are not transparent, the development of structures cannot be continuously monitored. Therefore, some of the experiments were repeated with a smaller amount of shortening (20%).

Modelling materials

One of the conditions for scaled models is that there must be rheological similarity between the original rock and the analogue modelling material (Hubbert 1937, Cobbold 1975, Baumann 1986, Weijermars & Schmeling 1986, Mancktelow 1988b). Paraffin wax has been used as an analogue material in many recent studies (e.g. Cobbold 1975, Latham 1979, Neurath & Smith 1982, Baumann 1986, Dixon & Simpson 1987, Odonne & Vialon 1987, Abbassi 1990, Abbassi & Mancktelow 1990). The rheology of the paraffin wax used in this study has been described recently in Mancktelow (1988b). Other descriptions of paraffin wax are given in Barry & Grace (1971), Cobbold (1975), Freund *et al.* (1982), Neurath & Smith (1982) and Abbassi (1990). These studies have shown that there are slight but significant differences in material properties even in

different lots from the same supplier. For this reason, each set of experiments should be performed with individually calibrated wax from the same lot.

In the models presented in this work, two different paraffin waxes were used. One with melting range (m.r.) 46–48°C for the matrix, the other one with melting range 50–52°C for the competent layer. Two sets of calibration experiments were performed corresponding to the temperature conditions of the model experiments: namely 24 ± 0.1 and 29 ± 0.1°C. The two waxes were calibrated at these temperatures using a rheometer ('Rhevisco') and the deformation rig. The wax used for the matrix (m.r. 46–48°C) has a power-law rheology with a stress exponent of $n \approx 3.7$ over the temperature range 24–25°C. Under the same conditions the layer (m.r. 50–52°C) has a stress exponent $n \approx 2.4$ (Mancktelow 1988a). In this temperature range (24–25°C) the waxes used for the matrix and the layer have an effective viscosity contrast of 17:1. Above 26–28°C, which approximates the α–β phase transition for the matrix (34°C for the layer), paraffin wax exhibits a sudden weakening (Mancktelow 1988a). At 29°C this results in very high viscosity contrast of about 600:1. A similar viscosity contrast was used in some experiments with analogue materials (e.g. Odonne & Vialon 1987). Such a high viscosity contrast of about 600:1 may be geologically reasonable (Biot 1961).

Model preparation

The paraffin wax used for the matrix was melted and poured into moulds containing a removable aluminium plate having the geometry of the initial folds. After cooling, the paraffin wax was cut and the aluminium plate removed. In the mean time, a 4 mm thick flat plate of paraffin wax of higher melting range was prepared. It was then heated in the incubator until soft and moulded between the preformed matrix blocks. In this way, the competent layer has the shape of parallel, cylindrical folds with the desired geometry and orientation. The model was then machined into its final shape (290 × 130 × 60 mm) and loaded into the deformation rig. The initial bonding between layer and matrix was very weak, corresponding to the assumption of *easy slip* between layer and matrix in some folding theories (e.g. Biot 1959, 1961). Nevertheless, it has been shown (Biot 1959, Smith 1975, Mancktelow & Abbassi 1992, fig. 5) that at high viscosity ratio (*ca* >100:1) there should be no significant difference in growth rate for the two extremes of perfect slip and perfect adherence between layer and matrix.

After experimental deformation, one half of the matrix was removed to allow the three-dimensional observation of the folded layer.

Initial fold curvature, tightness and size were varied to investigate the influence of the first-fold geometry on the interference patterns. The initial fold geometry is, therefore, not representative of the mechanical properties of matrix and layer during the experimental 'second-phase' deformation; this can also occur in nature due to changing metamorphic conditions and hence changing rock rheology.

EXPERIMENTAL RESULTS

Type 1 interference geometry

In this set of experiments, a series of pre-formed cylindrical folds were refolded with the compression direction Z acting parallel to the initial fold hinge direction, the intermediate axis Y perpendicular to its axial plane and the extension direction X parallel to the first-fold axial plane and perpendicular to its axis (Fig. 1). Using the notation of Ramsay (1967, p. 521) and Thiessen & Means (1980) this means $\alpha = 90°$, $\beta = 90°$ and $\gamma = 0°$. In other words the envelope of the initial folds was parallel to the YZ plane. Deformation of a planar layer with the same orientation provided a comparison with the geometry of second phase folds (Fig. 2a).

In the case of passive layer behaviour, the superposition of two generations of folds with the chosen orientation should result in pronounced dome and basin structures. The results of the experiments with different initial fold shapes (shown in Fig. 5) are presented in Fig. 3. From this figure it can be seen that the hinge curvature has less influence on the interference pattern than the other geometrical factors. Folds with similar wavelength and amplitude but different curvature (fold shapes 2C and 2F after Hudleston 1973a) result in similar interference patterns. Both kink and rounded folds were refolded into Type 2 interference patterns, in which both hinges and axial planes to initial folds are folded (Figs. 3a & b). The only difference is that the second-phase folds are less pronounced on rounded initial folds, with a correspondingly larger amount of layer-parallel strain (LPS). Of 36% bulk shortening, 21% was accommodated by LPS in the case of kink folds and 25% in rounded ones; this can be compared to the case of folding of the planar layer (Fig. 6), when there was only 1% LPS. In general, the LPS is larger in models giving

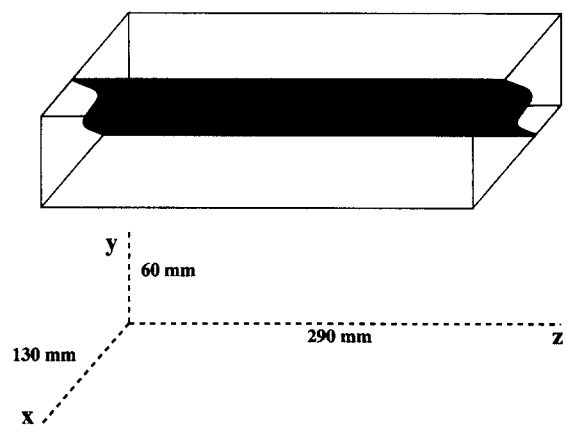

Fig. 1. Schematic diagram of models for Type 1 interference pattern strain geometry. The strain geometry refers to the orientation of the initial fold hinge and axial plane with respect to the XYZ bulk strain axes of the second deformation.

Type 2 interference patterns than in models with Type 1 interference patterns (Fig. 6).

The tightness of the initial folds exerts a very strong influence on the interference patterns that are formed. Open to close folds (interlimb angle 90°) refold into Type 2 interference patterns (with folding of the hinge in the *YZ* plane, and almost no folding of it in the *XZ* plane) (Fig. 3a); tight folds (interlimb angle 45°) refold into pronounced Type 2 interference patterns (Fig. 3c). In all these cases, the second-phase fold hinges are situated in the *XY* plane with their orientation depending on the orientation of the limbs of the initial folds (Ramsay 1967, pp. 539–540). With increasing tightness of the initial folds, second-phase fold axes approach the *X* axis, becoming parallel to it during refolding of isoclinal initial folds. This can be simulated by deformation of a planar single layer oriented parallel to the *XZ* plane (Fig. 2b).

With increasing interlimb angle of the initial folds, their hinges become folded in the *XZ* plane; the initial fold axial plane is no longer folded, resulting in Type 1 interference patterns. Dome and basin interference structures resulting from the refolding of gentle initial folds (interlimb angle 135°) are complicated by curvature-accommodation folds (Stauffer 1988, Lisle *et al.* 1990) (Fig. 3d). The wavelength of the second-phase folds is larger than the wavelength of folds developed in a single flat layer parallel to the *YZ* plane (Fig. 2a).

Similar observations on the influence of initial fold tightness and roundness have been made by Ghosh & Ramberg (1968), Skjernaa (1975), Watkinson (1981), Odonne & Vialon (1987) and Ghosh *et al.* (1992).

Initial folds with the same interlimb angle and the same hinge curvature can produce different interference patterns depending on their amplitude (A) or their *relative size*. This ratio is expressed here as the ratio of the amplitude of the initial folds to that of the virtual second-phase folds which would have developed if the layer were flat:

$$s = A_1/A_2.$$

Three experiments were performed. The initial fold shape was kept constant: that is, the initial folds had a kink shape and interlimb angle of 90°, but differed in size. The potential second-phase fold amplitude was A_2 = 21.1 mm. Large initial folds (s = 0.68) were refolded into Type 2 interference patterns, while small initial folds (s = 0.27) gave clear dome and basin structures (compare Figs. 3a and 3f). Intermediate initial folds (s = 0.44) had folded axial planes while their hinges were buckled sideways and upwards producing a combination of Types 1 and 2 interference patterns (Fig. 3e).

All the experiments were performed twice to test for reproducibility. The results were always the same: every type of second-phase structure was identified in both experiments. The only exception was the experiment with intermediate-size initial folds. Although all the second-phase structures are present in both experiments their magnitudes are not the same. In one experiment the Type 2 interference pattern is dominant while in the second one the dome and basin structures are better developed. This suggests that both possibilities are likely under the same geometrical and rheological conditions. Which structures will be better developed depends on which one initiates first, which in turn depends on the initial perturbations. In the case in which dome and basin structures dominate, those folds that refold the axial planes of the initial folds are situated only on dome culminations and basin depressions. This suggests that the dome and basin structures initiated first. During deformation, the limbs of these structures were rotated to a position where the maximum shortening acted obliquely to the layering and therefore obliquely to the initial fold hinges, whereas in broad second-phase hinge zones the maximum shortening acted parallel to the initial fold hinges; this strain was accommodated by sideways buckling.

One could ask what the changeover values of interlimb angle and fold arc length are for Type 1 or Type 2 interference patterns to occur. There is no unambiguous answer since these values depend largely on the rheology of the material and deformation boundary conditions: for the same strain and geometry of initial folds it will be easier to refold tighter and/or larger folds into dome and basin structures with increasing viscosity contrast. With a low viscosity contrast, it will be difficult for any refolding to occur. In this situation, independent of geometry of the initial folds, most of the strain will be accommodated by LPS. Where the viscosity contrast is relatively low, even in a flat layer, initial perturbations are required for the initiation of buckling (Abbassi & Mancktelow 1990).

Type 2 interference geometry

In the second group of experiments, the envelope of the initial folds was oriented parallel to the *XZ* plane (Fig. 7). In this strain geometry the compression direction was parallel to the initial fold hinges, the intermediate axis parallel to their axial planes and perpendicular to their hinges, and the extension direction perpendicular to the initial fold axial planes (α = 90°, β = 0°, γ = 0°). In this group of experiments, only the fold size has been varied (Fig. 8). Three different fold sizes were used as in the Type 1 interference geometry, but with different relative sizes since the second-phase folds in this strain geometry are smaller (A_2 = 16.1 mm).

For all three initial fold shapes, two models with identical initial fold geometry were deformed: the first with 36% bulk shortening, and the second with 20% bulk shortening. As in the first group of experiments, the largest initial folds (s = 0.9) were refolded into Type 2 interference patterns, intermediate folds (s = 0.58) were refolded into a combination of Types 1 and 2 interference patterns with Type 2 dominating (Figs. 4a & b), and small initial folds (s = 0.36) were refolded into clear dome and basin structures (Fig. 4c). These different patterns developed even though the imposed strain geometry was always that of Type 2 interference patterns. Comparing the initial stage with the 20%

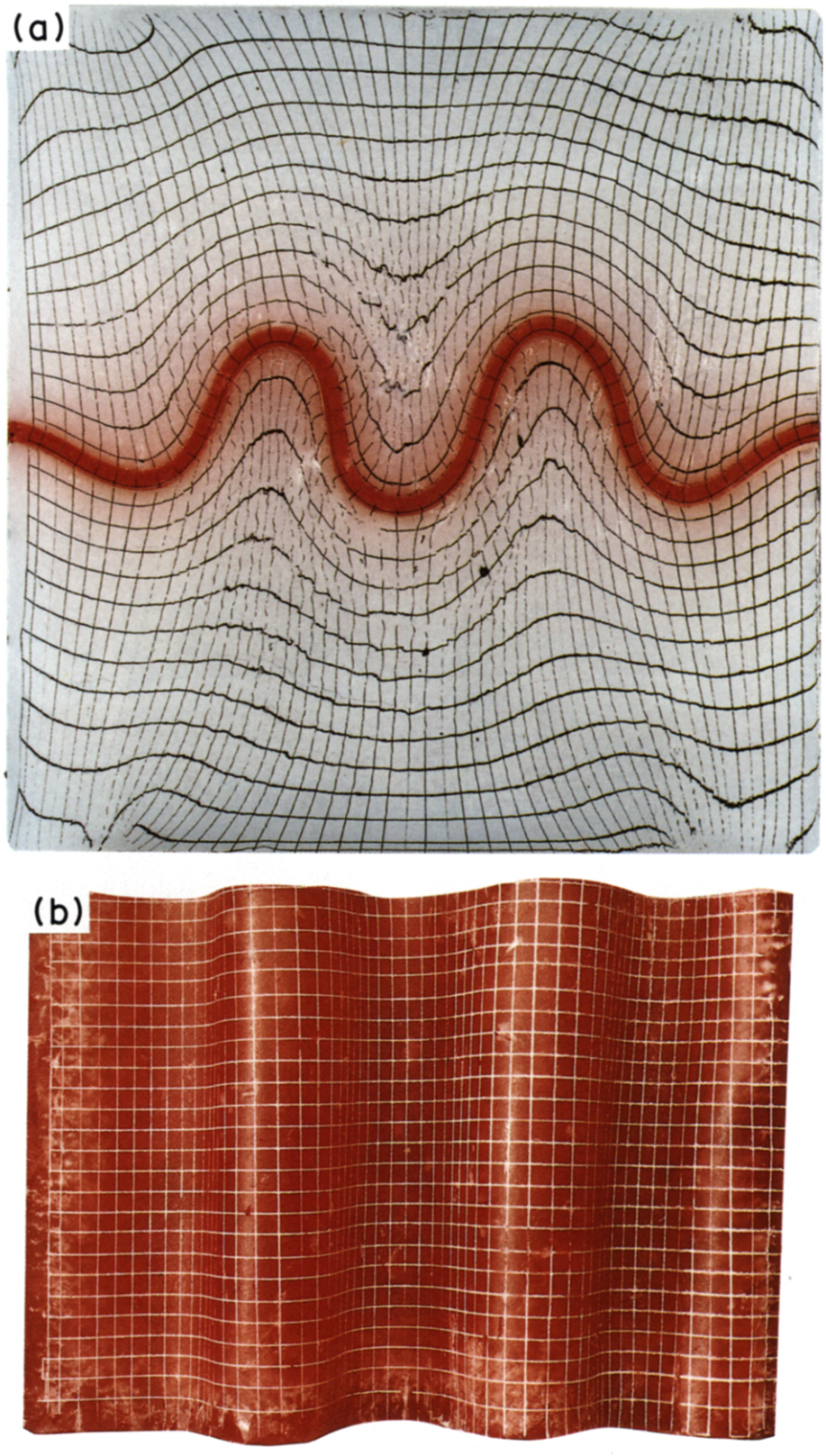

Fig. 2. Photographs of single-layer experiments, viewed in the XZ plane at 36% shortening. (a) Flat layer initially parallel to the YZ plane; (b) flat layer initially parallel to the XZ plane. The shortening direction is horizontal in both sub-figures.

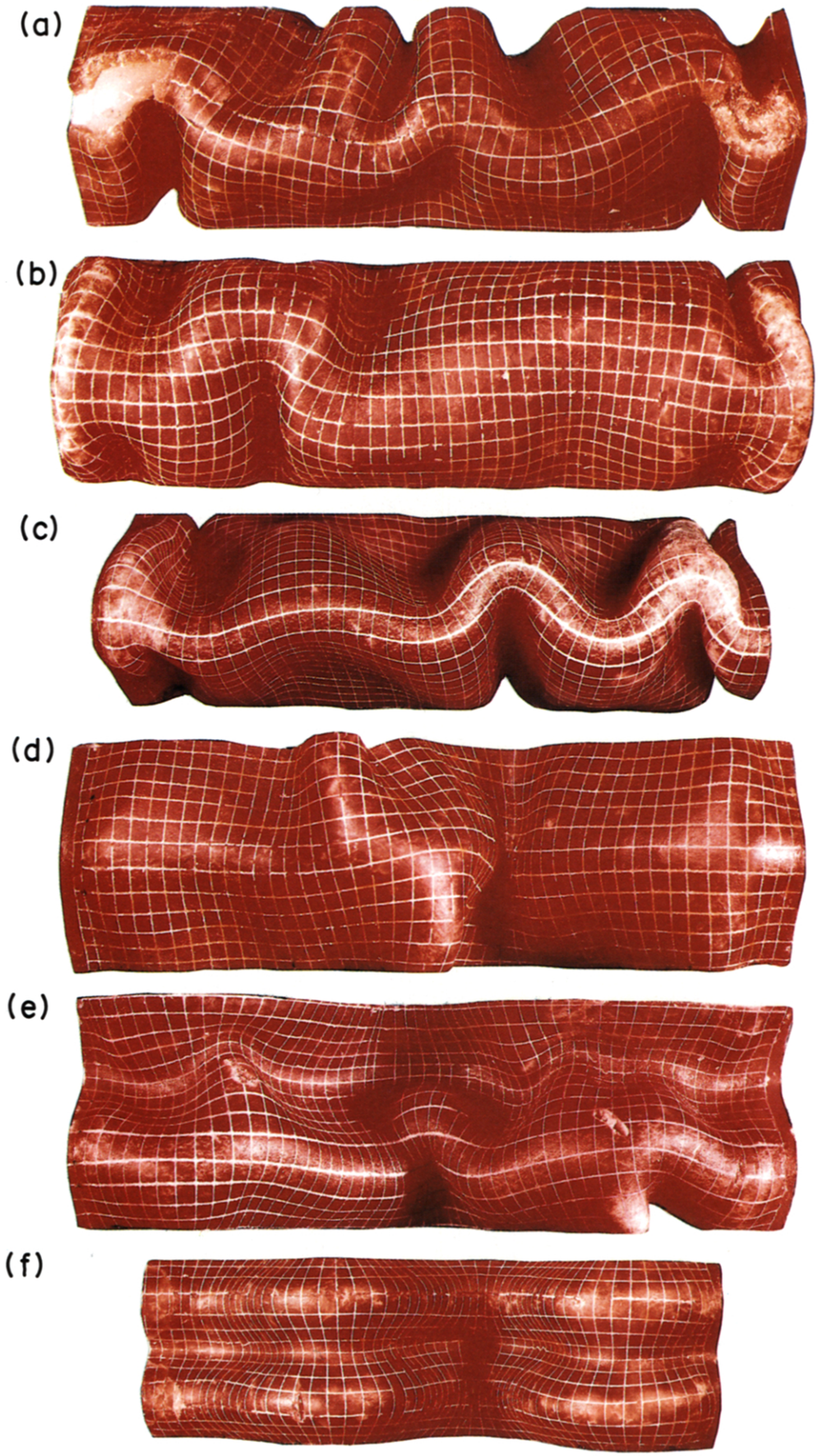

Fig. 3. Photographs of models deformed under Type 1 interference strain geometry at 36% shortening, seen in the YZ plane. The shape of the corresponding initial fold at 0% shortening is given in Fig. 5: (a) open, kink-shaped initial fold, initial amplitude A_0 = 14.4 mm, interlimb angle 90°; (b) rounded initial fold, A_0 = 30.2 mm; (c) tight, kink-shaped initial fold, A_0 = 62.5 mm, interlimb angle 45°; (d) gentle, kink-shaped initial fold, A_0 = 11.7 mm, interlimb angle 135°; (e) open, kink-shaped initial fold, A_0 = 9.23 mm, interlimb angle 90°; (f) open, kink-shaped initial fold, A_0 = 5.74 mm, interlimb angle 90°. In all models the longitudinal grid lines were originally parallel to the initial fold hinge. Spacing between grid lines is roughly 5 mm.

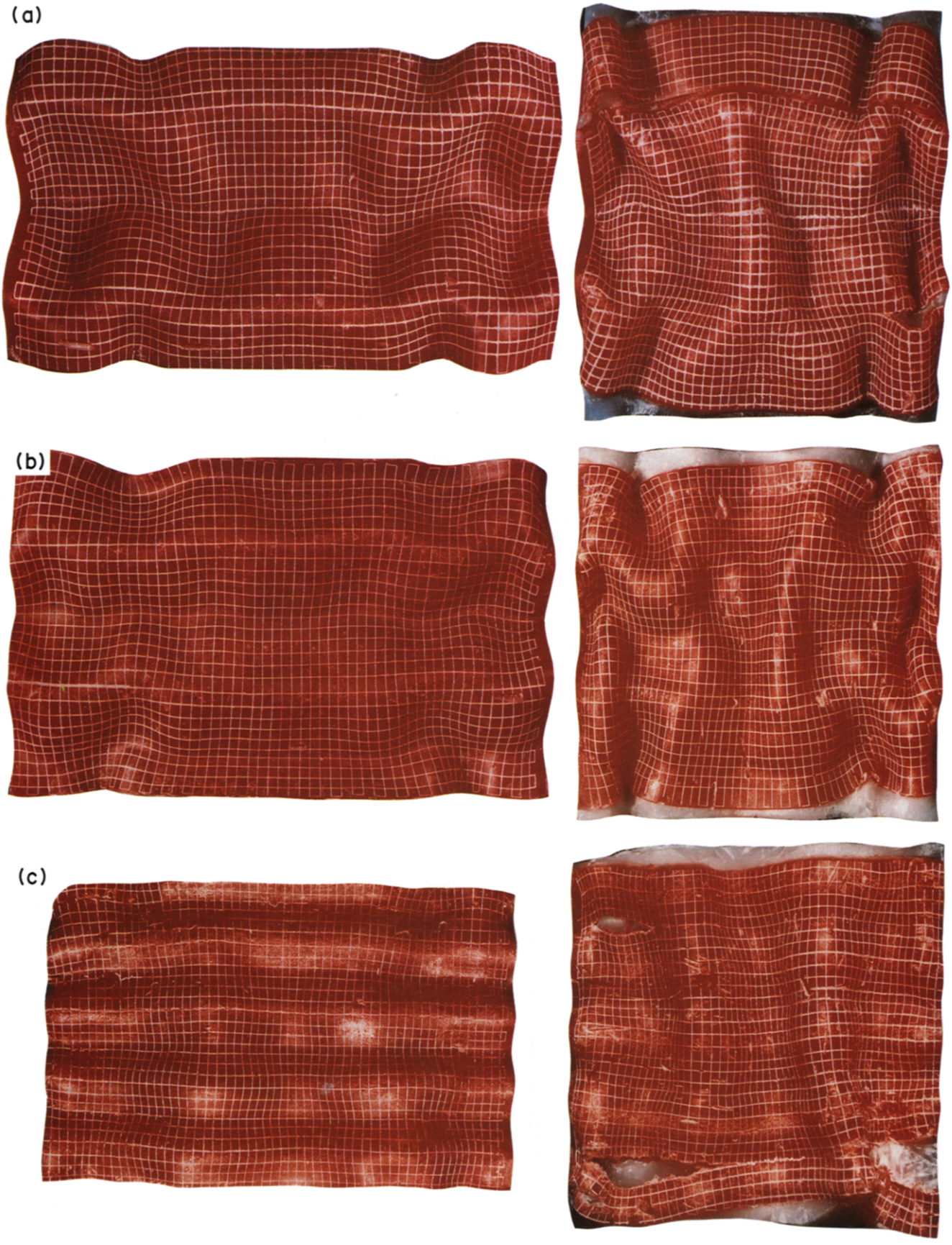

Fig. 4. Photographs of models deformed under Type 2 interference strain geometry at 20% (left) and 36% shortening (right), seen in the XZ plane. The shape of the corresponding initial fold at 0% shortening is given in Fig. 8. All initial folds were open, kink-shaped with interlimb angle 90°: (a) $A_0 = 14.4$ mm; (b) $A_0 = 9.23$ mm; (c) $A_0 = 5.74$ mm. In all models the longitudinal grid lines were originally parallel to the initial fold hinge. Spacing between grid lines is roughly 5 mm.

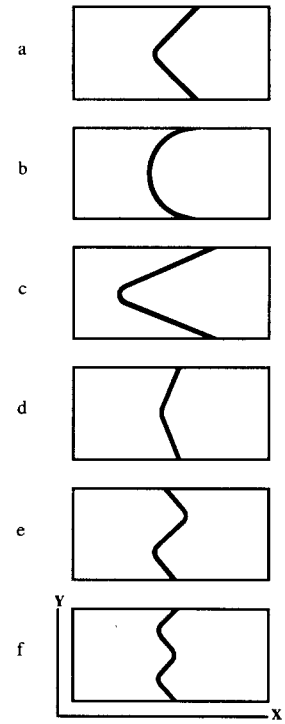

Fig. 5. Shapes of the initial folds in Type 1 interference strain geometry, seen in the XY plane at 0% shortening. Sub-figure labelling is the same as in Fig. 3.

shortened stage and with the final one, it can be concluded that the initial folds tend to unfold and deamplify due to the bulk stretch perpendicular to their axial planes. This change of geometry of the initial folds during their deformation can result in a change in the apparent interference pattern. After 36% shortening, the initial folds have a very low amplitude compared to

Y Initial fold shape Z	Experiment title	Interference type	% *LPS*
	RF901	none	1.0
	RW1901	2	21.0 (hinge) 17.0 (limbs)
	RC901	2	25.0
	RW45901	2	24.0 (hinge) 16.0 (limbs)
	RW135901	1	15.0 (hinge) 13.0 (limbs)
	RW2901	2+1 & 1+2	24.0 (hinge) 21.0 (limbs)
	RW3901	1	15.0

Fig. 6. Interference patterns and LPS for models deformed in Type 1 interference strain geometry. The amount of layer-parallel strain was calculated as: %LPS = $(l_0 - l_1)/l_0 * 100\%$, where l_0 and l_1 are the initial and deformed arc lengths measured from end-to-end along the layer (e.g. Hudleston 1973b, Abbassi & Mancktelow 1990).

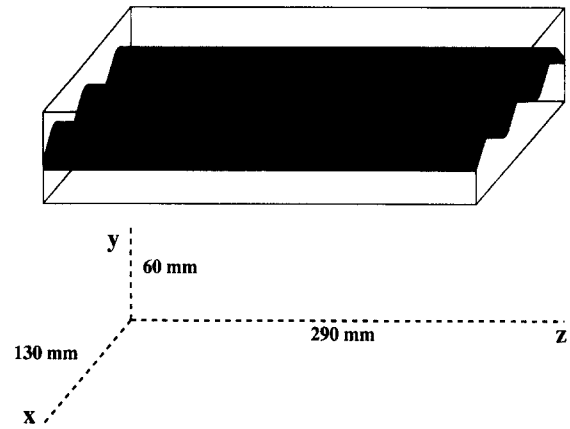

Fig. 7. Schematic diagram of models for Type 2 interference pattern strain geometry. The strain geometry refers to the orientation of the initial fold hinge and axial plane with respect to the XYZ bulk strain axes of the second deformation.

the superposed folds, but the distribution of second-phase folds will depend on the mode of buckling in the initial stages of deformation. The layer-parallel strain was very high (Fig. 9). After 20% shortening most of the strain in the Z direction was accommodated by layer-parallel shortening while in the X direction there was 9–10% layer-parallel stretching. Significant buckling occurred after this stage when the initial folds were more open. After 36% shortening the LPS in the Z direction was again the smallest in the model giving a Type 1 interference pattern, while in the other two cases it was between 24 and 27%. The layer-parallel stretching in the X direction (parallel to the superposed fold hinges) was between 15 and 20%.

In the refolding of the small initial folds, both initial folds and the superposed folds are equally developed at 20% shortening, giving Type 1 interference patterns, although the initial folds have been opened slightly. The axial planes of the second-phase folds are bowed in a mirror image way. With further deformation, the initial folds become very gentle, and superposed folds, therefore, amplify more easily. After 36% shortening the initial folds are almost completely unfolded. In some places, the unfolding could not keep pace with the stretching and boudins were formed. These occurred along the initial fold hinges and were controlled by

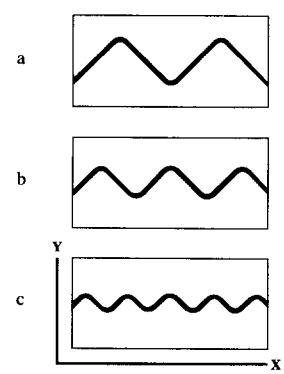

Fig. 8. Shapes of the initial folds in Type 2 interference strain geometry, seen in the XY plane at 0% shortening. Sub-figure labelling is the same as in Fig. 4.

Y / Initial fold shape / X	Shortening	Interference type	% LPS
	36%	none	(Z) 1.0
			(X) -4.0
	20%	2	(Z) 19.0
			(X) -8.6
	36%	2	(Z) 24.0
			(X) -15.0
	20%	2+1	(Z) 19.5
			(X) -9.3
	36%	2	(Z) 27.0
			(X) -16.0
	20%	1	(Z) 18.0
			(X) -10.0
	36%	1	(Z) 20.0
			(X) -20.0

Fig. 9. Interference patterns and LPS for models deformed in Type 2 interference strain geometry. Positive values of LPS indicate layer-parallel shortening while negative values of LPS indicate layer-parallel stretching.

microcracks along the outer arcs of the hinges. Boudins formed in this way lie in the XZ plane, parallel to the maximum shortening direction and normal to contemporaneous superposed fold hinges. They are not quite straight, and along their general trend they give the impression of being folded. Second-phase folds are well developed with similar, though shorter, wavelengths than second-phase folds formed by shortening the initially planar layer parallel to the XZ plane. They have less bowed axial planes and undulating hinges, which change their direction of plunge where they cross the now almost undetectable initial fold hinges.

Interference patterns on large and intermediate size initial folds are similar. At 20% shortening the initial axial planes are folded and their hinges buckled sideways. After 36% shortening the initial folds are unfolded and boudinaged in a similar manner to the previous case. The second-phase folds are well developed and distributed in a complex mode. On first appearance, they seem to be branching and to be distributed en échelon (Fig. 10a). But, when the stages at 20 and 36% shortening are compared, it can be seen that the same superposed folds on the two limbs of the initial fold change from anticline into syncline, and vice versa, after the unfolding of the initial fold. This change occurs along the same axial plane and where it passes from one limb of the initial fold to the other (Fig. 10b). The effect of changing the character of superposed folds is basically a result of 'unfolded' originally sideways-buckled initial folds.

Layer-parallel shortening and change in the geometry of initial folds

In Type 1 interference geometry, when the viscosity contrast was low (17:1), few or no second-phase folds were produced. Most of the 38% bulk shortening in the competent layer was taken up by layer-parallel strain (35.1%). This is similar to the LPS in the case of shortening the planar layer (under the same boundary conditions) parallel to the YZ plane (36.2%). In the XY plane, which corresponds to the section perpendicular to the initial fold axis, this shortening, since homogeneous, modifies the shape of the initial folds and leads to a

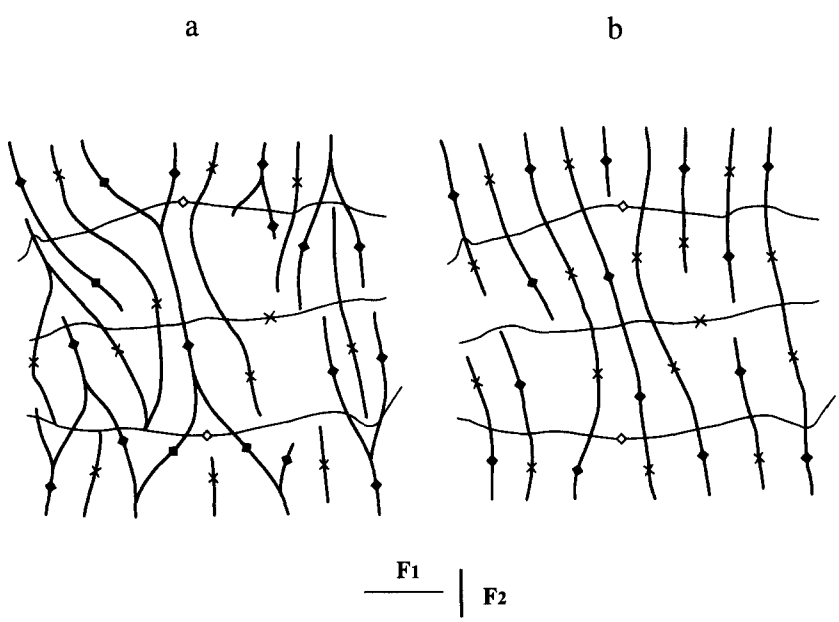

Fig. 10. Map views of model with initial fold amplitude of 9.23 mm deformed in Type 2 interference geometry at 36% shortening (Fig. 4b). (a) 'Classic' interpretation connecting anticlines with anticlines. Second-phase fold axial traces show branching and en échelon distribution; (b) interpretation in which the same folds are connected regardless of changes in facing direction along the strike of their axial planes. Second-phase folds change from anticline into syncline and vice versa when passing across initial fold hinges. Axial traces of such folds are more continuous than in the classic interpretation.

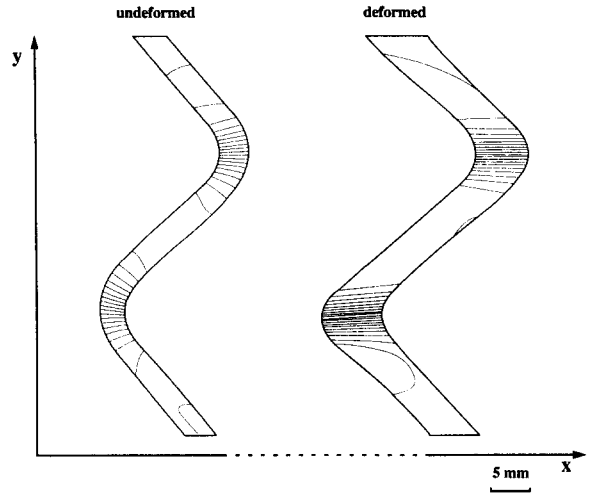

Fig. 11. Dip isogon plot of the initial fold with the same initial shape as the one in Fig. 5(e) but with a viscosity ratio of 17:1, at 0 and 36% shortening. Dip isogons at 5° intervals. Isogons are plotted using a program 'Isogon' by N. Mancktelow.

change in fold class from 1B (parallel) towards 2 (similar) (Figs. 11 and 12). In this way, nearly similar folds have been produced from originally parallel folds through shortening parallel to the fold axis in pure shear–plain strain conditions. This is an alternative model to the one from Ramsay (1962a), in which the similar folds develop by a mechanism of differential flattening or by flattening an initially parallel fold perpendicular to its axial plane. In nature, the shortening parallel to the initial fold axis could produce a second cleavage (e.g. crenulation cleavage) which transects folds with no obvious relation to higher-order superposed folds.

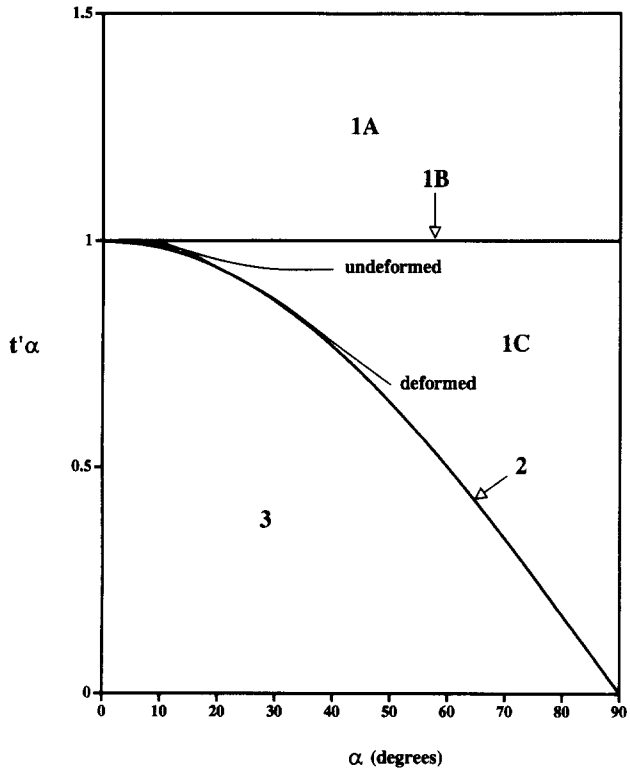

Fig. 12. Graphical plot of standardized orthogonal thickness t'_α plotted against angle of dip α for the initial fold represented in Fig. 11 at 0 and 36% shortening.

In experiments with high viscosity contrast (600:1), very little layer-parallel shortening is predicted by theory (e.g. Ramberg 1964), and experimentally-deformed, initially flat layers suffered only 1% LPS. The layer-parallel strain in models with initial folds was significantly larger, however, (cf. Figs. 6 and 9), due to structural *orthotropy* and a large *moment of inertia* (Troitsky 1976, p. 19) in the axial direction, and was dependent on the initial geometry. For elastic buckling of an unconfined corrugated plate the moment of inertia is related to the square of the corrugation amplitude and the inverse square of its tightness (A/W), while the flexural rigidity in the axial direction is linearly dependent on Young's modulus (Troitsky 1976, p. 81, Watkinson & Cobbold 1981). This implies that the LPS in superposed folding increases with increasing initial fold amplitude, decreases with increasing initial fold tightness and is dependent on viscosity contrast.

Hinge migration and transected folds

In all models in which Type 2 interference patterns developed, regardless of the strain geometry, migration of the initial fold hinges has been observed. The result is that what would be mapped as the folded first-fold hinge is no longer parallel to the line marked by points which were originally distributed along the initial fold hinge line. This line is less curved than the crest line and, in some cases, is almost straight in the YZ plane. The amount of hinge migration is greatest in the case of rounded initial folds, while, in the case of kink folds, it decreases with decreasing interlimb angle but is still always present (e.g. Figs. 3a–c).

The hinge migration proceeds in such a way that the crest migrates into the convex side of the superposed fold while the line defined by the initial fold hinge 'descends' in the concave side (Fig. 13). In this way the crest becomes buckled sideways while the original hinge line remains straighter and transects the crest at its inflection points. This effect is well recorded on the models with longitudinal grid lines originally parallel to the initial fold hinge line. After the deformation these longitudinal lines transect the apparent initial fold hinge. These grid lines are material ones and in nature they could, for example, represent the intersection lineation between layering and first axial-plane cleavage. Although this cleavage is initially axial planar, after refolding into Type 2 interference structures, it will transect the modified initial folds. The curvature of the axial plane, and therefore the curvature of the axial-plane cleavage is smaller than the curvature of the related limbs. This cleavage is no longer axial planar and the refolded folds are transected by their originally axial-planar cleavage.

DISCUSSION

The problem of folding two non-parallel planes has been already addressed by Ramsay (1963, p. 158, 1967,

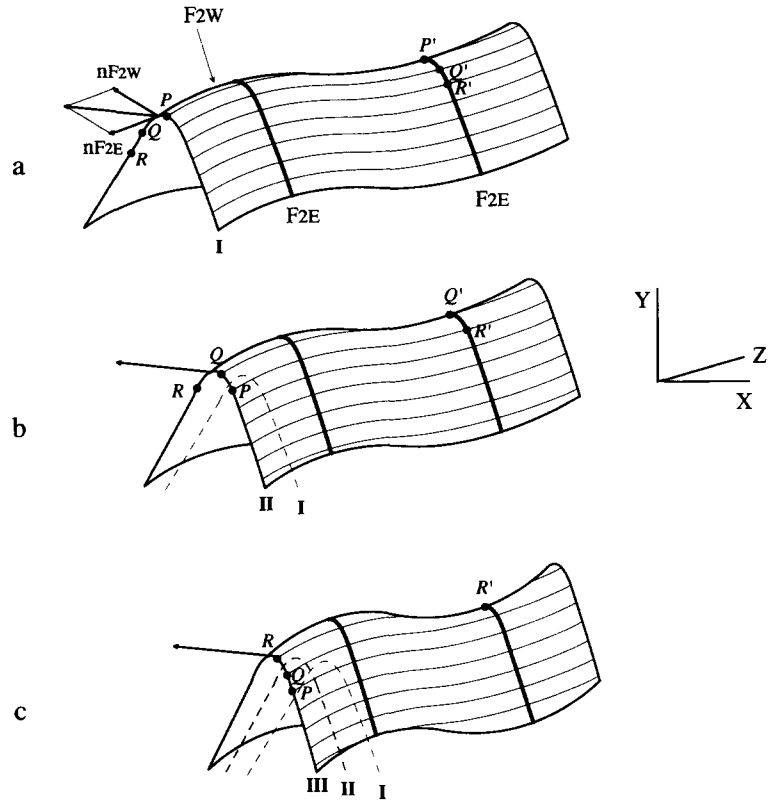

Fig. 13. Schematic diagrams of hinge migration: F_{2E}—second-phase fold axis on the east limb of the initial fold; F_{2W}—second-phase fold axis on the west limb of the initial fold; nF_{2E} and nF_{2W} are normals to F_{2E} and F_{2W}, respectively; P, Q, R and P′, Q′, R′ are points on the initial fold limb through which the initial fold hinge migrates in stages of superposed fold development I, II and III, represented in sub-figures (a), (b) and (c), respectively.

pp. 546–548) and Ramsay & Huber (1987, p. 489). It has been shown that independent buckling (by simple flexural slip or flexural flow) of the two limbs of the initial fold produces complex compatibility problems across the first fold's axial plane. Several models were proposed. Due to the rotating shearing motion on the surface separating the two initial fold limbs, the folded axial surface must develop into a slide. This sliding is probably easily accomplished along the initial axial-plane schistosity (if present). Where such schistosity is lacking, the strains can be adjusted by tightening of initial folds or by forming superposed folds by the mechanism of oblique flexural slip (Ramsay 1967, p. 396), or better by oblique flow buckling (Ramsay & Huber 1987, pp. 445 and 489). The current experiments show that other mechanisms are also possible.

In the case of sideways buckling, the sense of amplification of a superposed fold on the different limbs of the initial fold must be the same. It is contained in the common second axial plane and is parallel to the vector sum of the normals to the two second-phase fold axes (normals to the two limbs of the initial fold) (Fig. 13a). Consider the point P on the initial fold hinge where the two second-phase fold axes meet (fold axes on two limbs of the initial fold—F_{2E} and F_{2W} in Fig. 13). In the case of fold amplification perpendicular to its axis this point should move simultaneously in two directions for two second-phase fold axes (F_{2E} and F_{2W} in Fig. 13a). Since this is impossible, the resultant movement (amplification) direction is parallel to the direction of the vector sum of two potential directions, but the amplification rate of the superposed second-phase folds is smaller than that for independent, flat single layers. The superposed fold propagates through the initial fold like a wave and, therefore, by the next stage, the point Q will have moved to the crest line, whereas the point P will have descended into the convex–synclinal side of the superposed fold. Consequently, the initial fold hinge migrates in the direction of second-phase fold propagation. With increasing tightness of the initial folds, the amplification rate of the superposed folds will approach its maximum value. In other words, it is easier to refold tight initial folds into a Type 2 interference pattern than it is open ones. With increasing interlimb angle of initial folds, the resultant vector will tend to zero: it is impossible to buckle sideways folds with an initial interlimb angle of 180° (i.e. in-plane strain), but, with this geometry, upward buckling will obviously occur. The same rule applies for Type 1 interference patterns: an initial fold shortened parallel to its axis can potentially buckle both ways: sideways or upwards. Which one will prevail or which one will be dominant depends on the magnitudes of the two possible vectors. This means that an initial fold with interlimb angle of 90°, disregarding other factors, will have equal changes of being refolded into Type 1 or Type 2 interference patterns. This is true for both Type 1 and Type 2 imposed geometries (cf. Figs. 3 and 4).

The mutual relationship among factors influencing the buckling mode in the Type 1 strain geometry is

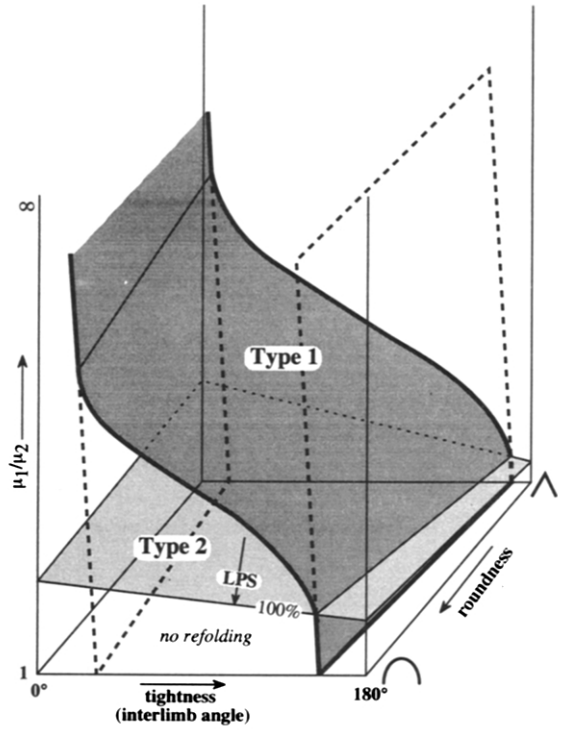

Fig. 14. The influence of shape factors on buckling mode. The lengths of the axes are not to scale.

represented schematically in Fig. 14. We have seen that the major factor is the initial fold size or rather the relative size of folds of the two generations. Fold size is a function of the viscosity ratio and, therefore, the interference pattern is primarily controlled by the viscosity ratio during the superposed deformation event. If we keep the initial fold size and shape constant but change the viscosity ratio in superposed folding we should observe the same control on the buckling mode as is provided by initial fold size with constant viscosity ratio. In Fig. 14 the vertical axis is the viscosity ratio. A similar diagram can be constructed for a particular viscosity ratio with relative fold size on the vertical axis. For the initial fold tightness, there is a minimum critical interlimb angle for which the initial fold will always buckle sideways since it approaches the geometry of a flat layer (isoclinal fold) parallel to the XZ plane. This angle decreases with increasing initial fold roundness and/or increasing viscosity ratio. Similarly, there is a maximum critical initial fold interlimb angle for which the initial fold will always buckle upwards, since it approaches the geometry of a flat layer (no initial folds) parallel to the YZ plane. This angle decreases with increasing initial fold roundness and/or increasing viscosity ratio. The partitioning of the bulk shortening between buckling (superposed folding) and LPS is a function of the effective layer thickness and therefore of initial fold shape. In the case of ideal cylindrical folds with no initial perturbation, there is a minimum viscosity ratio (for a particular initial fold shape) below which no superposed folding occurs, the whole strain being accommodated by LPS. The surface dividing the volumes where Type 1 or Type 2 interference occurs is constructed for plane strain; in a constrictional strain field it will move downwards because the upward buckling of initial folds is promoted by the relative increase in stretching perpendicular to the initial fold hinges. Below this surface only Type 2 interference patterns will develop because with decreasing viscosity ratio the superposed folds are smaller and, therefore, the relative size s is larger. Similarly, if the second-phase folds are large enough, the initial folds will be refolded into dome and basin structures independent of their shape. For a Type 2 interference geometry, this surface is situated higher since the two limiting planes, defined by the minimum and maximum initial fold interlimb angles, move to the right. Contrary to the previous case, the surface separating the two buckling mode volumes will move upwards in the constrictional strain field, because the maximum stretching direction is perpendicular to the initial fold axial planes and, therefore, sideways buckling is enhanced.

The above implies that the wavelength and growth rate of the second-phase folds will not be a simple function of viscosity but will itself be influenced by the shape and size of the initial folds (i.e. their moment of inertia). Although there is some variability, there is a clear proportionality to the wavelengths, consequently the viscosity ratio will still have a marked effect on folding (a linear variation of the flexural rigidity with elasticity) (cf. Troitsky 1976, Watkinson & Cobbold 1981).

CONCLUSIONS

Observations from the current experiments largely confirm the results of previous studies with similar boundary conditions. However, superposed folds, riding over rounded, open initial folds and forming a Type 1 interference pattern, such as those produced in experiments by Ghosh & Ramberg (1968), Skjernaa (1975) and Watkinson (1981), were not observed in this work. The reason could be the very high viscosity contrast between layer and matrix employed in the present study.

It has been shown that fold interference patterns are primarily controlled by the geometry of the initial folds, and to a lesser extent by the strain geometry. Among the shape factors, the major influence on the interference pattern (i.e. the buckling mode) is the initial fold amplitude: large folds refold into Type 2 interference patterns, smaller ones into Type 1 interference patterns. Where the initial folds are sufficiently small, relative to the superposed ones, they behave as linear markers. A secondary influence on the interference pattern is provided by the initial fold tightness: close to tight folds refold into Type 2, gentle to open ones into Type 1 interference patterns. In the present experiments, the initial fold roundness had only a limited effect.

The influence of the bulk strain is different for the first and second deformations. The magnitude of the superposed strain does not influence the buckling mode, i.e. the interference pattern. In the Type 1 strain geometry, the high superposed strain leads to pronounced interference patterns, both Type 1 and Type 2. For Type 2

interference geometry the high superposed strain leads to unfolding of initial folds and unclear interference patterns, but the initial buckling mode is still controlled by the initial fold geometry and viscosity ratio. On the other hand, the amount of strain during the first deformation influences the shape of the initial folds, and thus the interference pattern developed during the superposed deformation.

In the single layer experiments with an introduced perturbation (Abbassi & Mancktelow 1990, 1992, Mancktelow & Abbassi 1992), it has been shown that the presence of an initial perturbation in a single layer controls the location and the geometry of developing folds. Similarly, a perturbation in the initial folds in the sense of their non-cylindricity may be an additional factor in influencing the interference pattern. As shown by the experiment with the initial perturbation, when the viscosity ratio is high large initial perturbations are required to influence the geometry of the developing fold. In the same way, the initial folds should be highly non-cylindrical to influence the interference pattern. On the other hand, in natural rocks where the viscosity ratios are much lower, smaller amounts of non-cylindricity could be enough to control the interference patterns. The influence of such common irregularities on the interference pattern remains to be investigated.

Even in the case of a large viscosity ratio ($\approx$600:1), significant layer-parallel strain occurs in the direction of the initial fold hinges because of the large moment of inertia in the axial direction. Due to this large component of LPS, the shape of the initial fold changes towards a similar type.

During the sideways buckling of initial folds (Type 2 interference pattern), there are potentially large mechanical problems. In the experiments presented here, hinge migration occurred where layer-parallel strain along the hinge was larger than that along the limbs of the initial folds. This migration is largest in the case of rounded initial fold and smallest in tight, sharp ones.

Similar initial fold shapes will give the same interference patterns in different strain geometries although the detailed geometry (i.e. the final shape of the superposed folds) will be different. In Type 1 interference strain geometries, the initial folds will amplify and, in the case of high strain, pronounced interference structures can be produced. In contrast, with Type 2 strain geometries the initial folds will tend to de-amplify due to the stretching that occurs perpendicular to their axial planes. If the strain is high enough, initial folds can be obliterated and the superposed folds will be the dominating structures. Such folds are non-cylindrical but are less variable in plunge than those developed in Type 1 interference geometries. Furthermore, superposed folds change from antiforms into synforms where they pass through the initial fold hinges. In such places, the plunge of superposed structures can vary greatly, giving the (false) impression of a still younger deformational event.

The shape of superposed folds will be a function of the rheology of the deforming layer and the shape of the initial folds (which determine the buckling mode). Consequently, the shape and strain in the superposed folds will not be indicative of the mechanical properties of rocks during the superposed deformational event. In the same way, the modified initial folds no longer represent accurately the mechanical properties of the rocks during the first deformational event. In the Type 1 interference strain geometry, initial folds amplify and change their profile shape towards similar fold geometry while in the Type 2 interference strain geometry, initial folds de-amplify.

According to these observations, the type of interference pattern cannot *a priori* give as much information about the deformation history as is proposed by classic models of superposed folding by heterogeneous simple shear. A combined study of initial and superposed fold shape, axial directions, interference patterns, and strain is necessary in order to draw complete conclusions about the deformation history.

Acknowledgements—This paper represents part of a Ph.D thesis submitted to the ETH Zürich, and supervised by Neil Mancktelow and John Ramsay who substantially improved an earlier version of the manuscript by their critical reviews. Comments and discussions by Martin Casey and John Watkinson are much appreciated. Peter Hudleston, Mel Stauffer and an anonymous referee are thanked for helpful reviews, Mohammad Abbassi and Benoît Ildefonse introduced me to the analogue model techniques and Robert Hofmann provided the technical support during the experimental work. Margie Mancktelow improved the English. I would like to thank them all very much for their help. The financial support from the ETH Credits Nos 0-20-154-86 and 0-12-405-91 is gratefully acknowledged.

REFERENCES

Abbassi, M. R. 1990. Die Geometrie der initialen Perturbation und ihr Einfluss auf Faltenentwicklung. Unpublished Ph.D. thesis, ETH, Zürich, Switzerland.

Abbassi, M. R. & Mancktelow, N. S. 1990. The effect of initial perturbation shape and symmetry on fold development. *J. Struct. Geol.* **12**, 273–282.

Abbassi, M. R. & Mancktelow, N. S. 1992. Single layer folding in non-linear materials—I. Experimental study of fold development from an isolated initial perturbation. *J. Struct. Geol.* **14**, 85–104.

Barry, B. W. & Grace, A. J. 1971. Rheological properties of white soft paraffin. *Rheol. Acta* **10**, 113–120.

Baumann, M. T. 1986. Verformungverstelung an Scherzonenenden: Analogmodelle und natürliche Beispile. Unpublished Ph.D. thesis, ETH, Zürich, Switzerland.

Biot, M. A. 1959. On the instability and folding deformation of a layered viscoelastic medium in compression. *J. appl. Mech.* **E26**, 393–400.

Biot, M. A. 1961. Theory of folding of stratified viscoelastic media and its implication in tectonics and orogenesis. *Bull. geol. Soc. Am.* **72**, 1595–1620.

Charlesworth, H. A. K. 1987. Computer-constructed diagrams of folded and thrust-faulted strata. *J. Struct. Geol.* **9**, 503–504.

Cobbold, P. R. 1975. Fold propagation in single embedded layers. *Tectonophysics* **27**, 333–351.

Dixon, J. M. & Simpson, D. G. 1987. Centrifuge modelling of laccolith intrusion. *J. Struct. Geol.* **9**, 87–103.

Freund, M., Csikós, R., Keszthelyi, S. & Mózes, G. 1982. *Paraffin Products*, Elsevier, Amsterdam.

Ghosh, S. K. 1970. A theoretical study of intersecting fold patterns. *Tectonophysics* **9**, 559–569.

Ghosh, S. K. 1974. Strain distribution in superposed buckling folds and the problem of reorientation of early lineations. *Tectonophysics* **21**, 249–272.

Ghosh, S. K., Mandal, N., Khan, D. & Deb, S. K. 1992. Modes of superposed buckling in single layers controlled by initial tightness of early folds. *J. Struct. Geol.* **14**, 381–394.

Ghosh, S. K. & Ramberg, H. 1968. Buckling experiments on intersecting fold patterns. *Tectonophysics* **5**, 89–105.

Hubbert, M. K. 1937. Theory of scale models as applied to the study of geologic structures. *Bull. geol. Soc. Am.* **48**, 1459–1520.

Hudleston, P. J. 1973a. Fold morphology and some geometrical implications of theories of fold development. *Tectonophysics* **16**, 1–46.

Hudleston, P. J. 1973b. An analysis of 'single-layer' folds developed experimentally in viscous media. *Tectonophysics* **16**, 189–214.

Latham, J.-P. 1979. Experimentally developed folds in a material with a planar mineral fabric. *Tectonophysics* **57**, T1-T8.

Lisle, R. J., Styles, P. & Freeth, S. J. 1990. Fold interference structures: the influence of layer competence contrast. *Tectonophysics* **172**, 197–200.

Mancktelow, N. S. 1988a. An automated machine for pure shear deformation of analogue materials in plane strain. *J. Struct. Geol.* **10**, 101–108.

Mancktelow, N. S. 1988b. The rheology of paraffin wax and its usefulness as an analogue for rocks. *Bull. geol. Inst. Univ. Uppsala N.S.* **14**, 181–193.

Mancktelow, N. S. & Abbassi, M. R. 1992. Single layer buckle folding in non-linear materials—II. Comparison between theory and experiment. *J. Struct. Geol.* **14**, 105–120.

Neurath, C. & Smith, R. B. 1982. The effect of material properties on growth rates of folding and boudinage: experiments with wax models. *J. Struct. Geol.* **4**, 215–229.

O'Driscoll, E. S. 1962a. Experimental patterns in superimposed similar folding. *J. Alberta Soc. Petrol. Geol.* **10**, 145–167.

O'Driscoll, E. S. 1962b. Fold interference patterns in model experiments. *Nature* **193**, 115–117.

O'Driscoll, E. S. 1962c. Models for superposed laminar flow folding. *Nature* **196**, 1146–1148.

O'Driscoll, E. S. 1962d. Shape criteria in cross folding. *Aust. Oil & Gas. J.* **9**, 42–47.

O'Driscoll, E. S. 1964a. Cross fold deformation by simple shear. *Econ. Geol.* **59**, 1061–1093.

O'Driscoll, E. S. 1964b. Interference patterns from inclined shear fold system. *Bull Can. Petrol. Geol.* **12**, 279–310.

Odonne, F. 1987. Migrations de charnières et vecteurs de déplacement sur des modèles analogiques de plis superposés. *Geodinamica Acta* **1**, 139–146.

Odonne, F. & Vialon, P. 1987. Hinge migration as a mechanism of superimposed folding. *J. Struct. Geol.* **9**, 835–844.

Perrin, M., Oltra, P. H. & Coquillart, S. 1988. Progress in the study and modelling of similar fold interferences. *J. Struct. Geol.* **10**, 593–605.

Ramberg, H. 1964. Selective buckling of composite layers with contrasted rheological properties, a theory for simultaneous formation of several orders of folds. *Tectonophysics* **1**, 307–341.

Ramberg, H. 1981. *Gravity, Deformation and the Earth's Crust.* Academic Press, London.

Ramsay, J. G. 1962a. Interference patterns produced by the superposition of folds of similar types. *J. Geol.* **70**, 466–481.

Ramsay, J. G. 1962b. The geometry and mechanics of formation of "similar" type folds. *J. Geol.* **70**, 309–327.

Ramsay, J. G. 1963. Structure and metamorphism of the Moine and Lewisian rocks of the North West Caledonides. In: *The British Caledonides*. Oliver & Boyd, Edinburgh, 143–175.

Ramsay, J. G. 1967. *Folding and Fracturing of Rocks*. McGraw-Hill, New York.

Ramsay, J. G. & Huber, M. I. 1987. *The Techniques of Modern Structural Geology, Volume* 2: *Folds and Fractures*. Academic Press, London.

Reynolds, D. L. & Holmes, A. 1954. The superposition of Caledonoid folds on the older fold-system in the Dalradians of Malin Head, Co. Donegal. *Geol. Mag.* **91**, 417–433.

Skjernaa, L. 1975. Experiments on superimposed buckle folding. *Tectonophysics* **27**, 255–270.

Smith, R. B. 1975. Unified theory of the onset of folding, boudinage, and mullion structure. *Bull. geol. Soc. Am.* **86**, 1601–1608.

Stauffer, M. R. 1988. Fold interference structures and coaption folds. *Tectonophysics* **149**, 339–343.

Thiessen, R. L. 1986. Two dimensional refold interference patterns. *J. Struct. Geol.* **8**, 563–573.

Thiessen, R. L. & Means, W. D. 1980. Classification of fold interference patterns: a re-examination. *J. Struct. Geol.* **2**, 311–316.

Troitsky, M. S. 1976. *Stiffened Plates. Bending, Stability and Vibrations*. Elsevier, Amsterdam.

Watkinson, A. J. 1981. Patterns of fold interference: influence of early fold shapes. *J. Struct. Geol.* **3**, 19–23.

Watkinson, A. J. & Cobbold, P. R. 1981. Axial direction of folds in rocks with linear/planar fabrics. *J. Struct. Geol.* **3**, 211–217.

Weijermars, R. & Schmeling, H. 1986. Scaling of Newtonian and non-Newtonian fluid dynamics without inertia for quantitative modelling of rock flow due to gravity (including the concept of rheological similarity). *Phys. Earth & Planet. Interiors* **43**, 316–330.